INTERACTION FORCES BETWEEN RED CELLS AGGLUTINATED BY ANTIBODY

II. Measurement of Hydrodynamic Force of Breakup

SUSAN P. THA, JOSEPH SHUSTER AND HARRY L. GOLDSMITH
McGill University Medical Clinic, Montreal General Hospital Research Institute, Montreal, Quebec H3G 1A4, Canada

ABSTRACT The expressions derived in the previous paper for the respective normal, F_3, and shear forces, F_{shear}, acting along and perpendicular to the axis of a doublet of rigid spheres, were used to determine the hydrodynamic forces required to separate two red cell spheres of antigenic type B crosslinked by the corresponding antibody. Cells were sphered and swollen in isotonic buffered glycerol containing 8×10^{-5} M sodium dodecyl sulfate, fixed in 0.085% glutaraldehyde, and suspended in aqueous glycerol (viscosity: 15–34 mPa s), containing 0.15 M NaCl and anti-B antibody from human hyperimmune antiserum at concentrations from 0.73 to 3.56 vol%. After incubating and mixing for 12 h, doublets were observed through a microscope flowing in a 178-μm tube by gravity feed between two reservoirs. Using a traveling microtube apparatus, the doublets were tracked in a constantly accelerating flow and the translational and rotational motions were recorded on videotape until breakup occurred. From a frame by frame replay of the tape, the radial position, velocity and orientation of the doublet were obtained and the normal and shear forces of separation at breakup computed. Both forces increased significantly with increasing antiserum concentration, the mean values of F_3 increasing from 0.060 to 0.197 nN, and F_{shear} from 0.023 to 0.072 nN. There was no significant effect of glycerol viscosity on the forces of separation. It was not possible to determine whether the shear or normal force was responsible for doublet separation. Measurements of the mean dimensionless period of rotation, $\overline{TG}$, of doublets in suspensions containing 0.73 and 2.40% antiserum undergoing steady flow were also made to test whether the spheres were rigidly linked or capable of some independent rotation. A fairly narrow distribution in $\overline{TG}$ about the value 15.64, predicted for rigidly-linked doublets, was obtained at both antiserum concentrations.

INTRODUCTION

The preceding paper (Tha and Goldsmith, 1986) described the theoretical model of a rigid doublet of spheres having a fixed interparticle distance subjected to shear flow, and derived expressions for the normal and shear forces acting respectively along and perpendicular to the axis of the doublet. In the present paper, the analysis is used to determine the hydrodynamic forces required to separate two red blood cell (rbc) spheres of antigenic type B crosslinked by the corresponding antibody. The approach was to subject suspensions of sphered, swollen red cells in aqueous glycerol containing antiserum to flow in a 178-μm diameter tube. Doublets, formed by collisions between single cells, were observed through a microscope and then tracked and videotaped in a uniformly accelerating flow until breakup. From a frame by frame replay of the video tape, the shear rate and orientation angles of the doublet axis at the time of breakup were determined. The normal force, F_3, and the shear force, F_{shear}, were then calculated using:

$$F_3 = 19.33\eta G b^2 \sin^2\theta_1 \sin 2\phi_1, \quad (1)$$

$$F_{shear} = 7.02\eta G b^2\{(\cos 2\theta_2 \cos\phi_2)^2 + (\cos\theta_2 \sin\phi_2)^2\}^{1/2} \quad (2)$$

which were derived in Part I.[1] Measurements of the period of rotation, T, of the doublets were also made in order to test whether the spheres were rigidly linked or capable of some independent rotation.

EXPERIMENTAL PROCEDURES

Preparation of Swollen Sphered Red Blood Cells

Theoretical considerations require that the particles be spherical and rigid, i. e., undeformable under experimental conditions. Previous work using Evans blue as a sphering agent (Goldsmith et al., 1981; 1982) demonstrated the necessity of simultaneously swelling and sphering the

Dr. Tha was a fellow of the Medical Research Council of Canada 1980–1985.
Dr. Goldsmith is a Career Investigator of the Medical Research Council of Canada.
Address offprint requests to Dr. Goldsmith.

[1]The same system of nomenclature is used as in Part I of this paper. Symbols for Parts I and II are listed in the Glossary section of Part I.

rbc in order to diminish the asperities which, because of geometric considerations, are present when cells are sphered at constant volume. These asperities could reach up to hundreds of nanometers in length, and lead to departures from sphericity sufficient to affect the sphere trajectories during collision. Therefore, a new method using sodium dodecyl sulfate (SDS), glycerol, and glutaraldehyde in order respectively to sphere, swell, and harden the rbc was developed.

Blood was obtained by venipuncture from healthy volunteers in tubes containing EDTA. It was typed and then washed six times in 20 volumes of ice-cold isotonic phosphate buffer (PB) containing 1 mM Mg^{++} at pH 7.4 in order to remove the buffy coat and as much plasma protein as possible. 1 ml of packed rbc was abruptly added to 106 ml of stirred solution consisting of 100 ml glycerol buffer (18.42 g glycerol and 333 ml PB/l) and 6 ml of 0.00173 M SDS. After 12 s, prior to any hemolysis of the cells, 10 ml of glutaraldehyde 1% (J.B.EM Services, Inc., Pointe Claire, Québec) was added, the final concentration of glutaraldehyde being 0.085%. The mixture was stirred for 12 min, then washed 6 times in PB. The cells were stored at 4°C in PB with sodium azide 0.05%, conditions in which they were stable to aggregation for many weeks. All cells used in this set of experiments were of type B.

This treatment usually results in no hemolysis of rbc. Less than 1% of cells were aggregated. The cells appeared perfectly spherical under light microscopy at 1,200 × magnification. Scanning and transmission electron microsopy (Fig. 1) showed cells of high sphericity and some surface asperities. The mean cell diameter, from videotape analysis of a population of 300 cells, was 6.42 ± 0.30 μm SD. They exhibited no change in shape or volume in distilled water or concentrated glycerol solutions.

For the flow studies, an rbc antiserum suspension was prepared as follows: the sphered, swollen rbc were washed and diluted in PB such that 30 μl of cell suspension would yield a final concentration of 2.5 ± 10^4 cells/μl in the flow suspension. The flow suspension consisted of 2 ml of glycerol 67–76% w/w in 0.15 M NaCl, to which was added 30 μl of rbc suspension and 15–75 μl of the appropriate antiserum (Ortho Diagnostics Systems, Inc., Don Mills, Ont.), yielding a final antiserum concentration of 0.73–3.56 vol% (dilutions of 1/137 to 1/28.1). The flow suspension was allowed to equilibrate for 12 h at 22°C on a rotary mixer at 3 rpm. On some occasions it was then centrifuged at 125 *g* for 25 min and gently redispersed before slowly injecting it into the flow system.

This treatment resulted in the formation of considerable numbers of doublets, as well as a few triplets and quadruplets of cells, the latter being more plentiful at higher antiserum concentrations. There were almost no aggregates consisting of five or more cells.

Flow System

This is depicted in Fig. 2. The flow suspension was observed in a microtube consisting of a 5-cm length of precision bore glass tubing of 178 μm i. d. (Wilmad Glass Co., Inc., Buena, NJ). The upstream end was connected to an 0.5-cm length of 500 μm i. d. glass tubing which was hand-drawn over a flame to narrow abruptly to fit the microtube in order that cells be subjected to minimal shearing prior to being tracked in the flow tube. The tubes were mounted on a 5.0 × 7.5-cm microscope slide on which a viewing chamber surrounding the microtube was constructed. This chamber was filled with the same glycerol solution as that in the microtube in order to minimize optical distortion. The tubes were attached upstream by a 17-gauge stainless steel needle and connector to a 30-cm length of polyethylene tubing (PE 205; i. d. = 1.57 mm), and downstream by a 17-gauge needle to a 20-cm length of tubing (PE 100; i. d. = 0.86 mm). The PE 100 tubing was attached to a Teflon hub into which was inserted an amputated 3-ml plastic syringe open to the atmosphere which served as the collection reservoir. The PE 205 tubing was connected by a Teflon hub to a 10-ml glass pipette which served as the infusion reservoir.

The entire microtube assembly was then placed on a jig for mounting

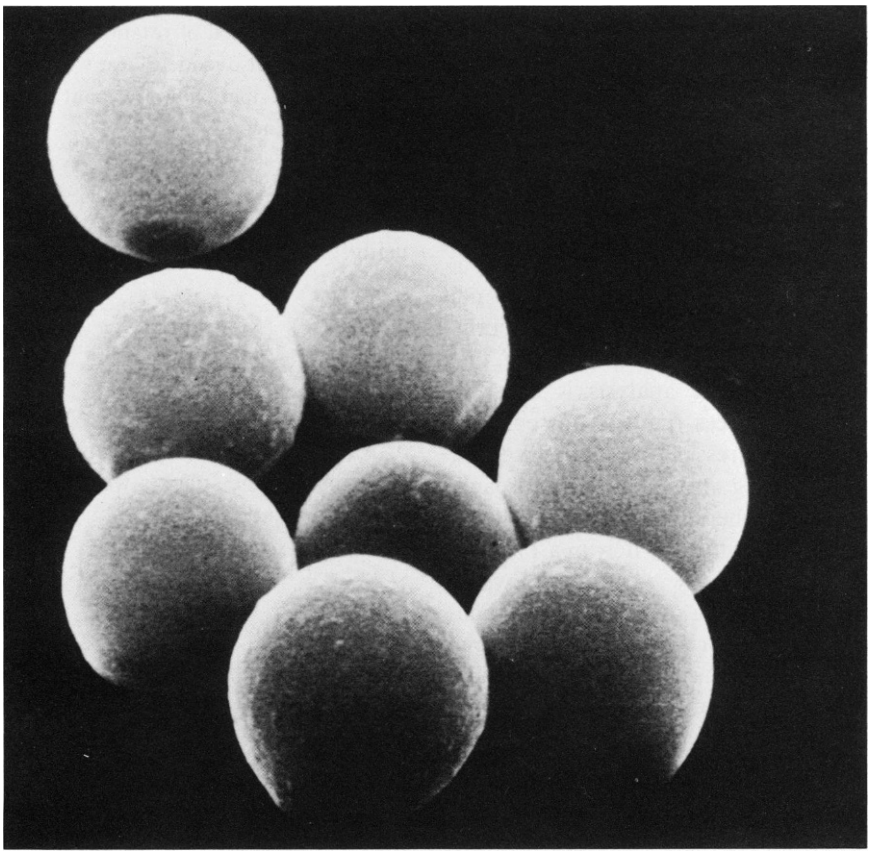

FIGURE 1 Scanning electron micrographs of sphered and swollen human red cells. 6,020×.

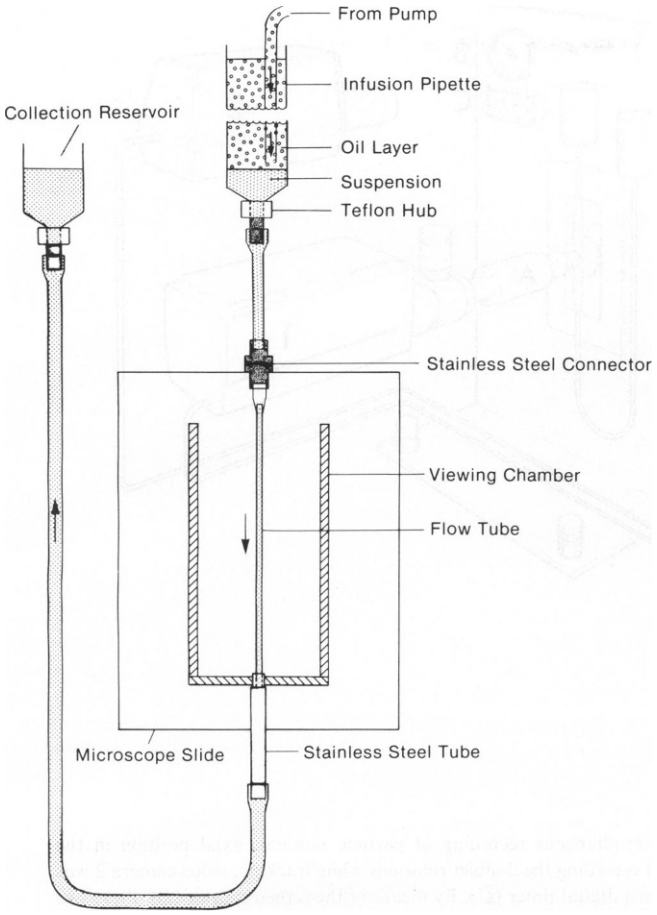

FIGURE 2 The flow system. The suspension of red cells in glycerol flowed through the 178-μm tube by gravity feed between two reservoirs. The tube lay on a microscope slide mounted on a jig on the hydraulically-driven stage of the traveling microtube apparatus. The flow rate was uniformly accelerated by infusing silicone oil into the pipette infusion reservoir, and doublets tracked down the tube by moving the stage upward with continually increasing velocity.

on the traveling microtube apparatus previously described (Vadas et al. 1973; Goldsmith and Mason, 1975). The jig was mounted on a vertically positioned sliding platform with a built-in microscope stage. The platform was driven by the piston of the slave cylinder of a hydraulic microdrive; the master cylinder was driven via a micrometer screw by a continuously variable D.C. motor. The maximum speed of the platform, and consequently the maximum velocity at which a particle could be tracked, was ~920 μm s^{-1}. An odometer connected to the platform measured distance in 10-μm increments. The traveling microtube apparatus rested on a vibration-free air-cushioned table.

Doublet Breakup

Tracking and recording. The flow suspension underwent gravity flow by adjustment of the relative height of the two reservoirs. Initially, the suspension was subjected to volumetric flow rates $Q \simeq 0.25$ μl h^{-1} corresponding to a fluid centerline velocity $u_3(0) \simeq 5$ μm s^{-1}. When a doublet was seen entering the microtube, the flow rate was accelerated at a rate of ~12.5 μm s^{-2} by infusing silicone oil into the pipette from a Harvard pump. A doublet could thus be tracked from its entry into the microtube, usually at velocities of 1–3 μm s^{-1}; the flow was then accelerated and the doublet tracked until breakup or until its velocity exceeded the maximum speed of the stage.

The flow suspensions were viewed in the median plane of the microtube through a horizontally positioned monocular microscope (Carl Zeiss, Inc., Thornwood, NY) along a fixed optical axis normal to the microtube. A 40 × objective and a 16 × eyepiece were used. Bright field illumination was provided with a 150 W xenon arc.

As previously described (Takamura et al., 1979), the motion of a doublet was viewed with a videocamera (model AVC-1400, Sony Canada, Ltd., Montreal) attached to the microscope; simultaneously a second Sony videocamera was trained on the odometer (Fig. 3). The two images were recorded on the same frame using a screen-splitter (Thalner Electronics, MI) by a videorecorder (model NV-8950, Panasonic Canada, Mississauga, Ontario) at 30 frames s^{-1} and displayed on a 15" monitor (model V19-121, Electrohome Ltd., Kitchener, Ontario). As the videorecorder was capable of frame-by-frame replay, the velocity of a doublet could be determined by measuring the distance elapsed on the odometer per frame, i. e., per 33.3 ms. On some occasions a stop watch placed beneath the odometer was also recorded for backup.

Method of analysis. To derive the normal and shear forces, the variables of Eqs. 1 and 2 [G, b, η, (θ_1, ϕ_1), and (θ_2, ϕ_2)] must be extracted from the recorded motion of a doublet. In a dilute suspension of particles undergoing Poiseuille flow, providing $b/R_o \ll 1$, it has been shown that the particle velocity $v_3(R)$ in the axial, x_3, direction, at a radial distance R from the tube axis (Fig. 1 *a* of the preceding paper [Tha and Goldsmith, 1986]) is equal to that of the fluid, $u_3(R)$, (Goldsmith and Mason, 1962):

$$v_3(R) = u_3(R) = u_3(0)\left[1 - \frac{R^2}{R_o^2}\right]. \tag{3}$$

The shear rate at a radial distance R is given by:

$$G(R) = \frac{2u_3(0)}{R_o^2}R, \tag{4}$$

$$= \frac{2u_3(R)R}{R_o^2 - R^2}, \tag{5}$$

using Eq. 3.

In the experiments, $v_3(R)$ was determined by frame-by-frame playback of the doublet motion during the sequence of breakup. The velocity was measured over a distance on the odometer corresponding to 10 to 15 frames or 0.33 to 0.50 s, the breakup occurring at the midpoint of the sequence.

The radial distance R was measured with the aid of a digital videoposition analyzer (model VPA-1000, FOR-A Co. Ltd., Tokyo) whose projection was superimposed on the videorecorder image. The video analyzer was calibrated with a micrometer scale. Previous work has shown that the inner wall of the microtube is visible as a thin white line on the axial side of a band of internal reflection (Goldsmith and Marlow, 1972). The video analyzer measured the radial distance $(R_o - R)$ from the center of the doublet to the tube wall from which R was obtained using the value of R_o independently determined with a Leitz micrometer ocular.

The radius b of the rbc was obtained from the video analyzer's measurement of the diameters of the spheres. No doublet was analyzed in which b for the two cells was measurably discrepant.

The orientation angles θ_1 and ϕ_1 of the doublet axis, as shown in Figs. 1 *a* and 2 of the preceding paper, were estimated as follows: assuming that the doublets rotate as prolate ellipsoids, the θ_1 orientation of the axis is given by integration of Eq. 2 of the preceding paper (Jeffery, 1922),

$$\tan\theta_1 = \frac{Cr_e(r^*)}{(r_e^2(r^*)\cos^2\phi_1 + \sin^2\phi_1)^{1/2}}, \tag{6}$$

where C is the orbit constant ($C = \infty$ at all ϕ_1 when $\theta_1 = \pi/2$), and $r_e(r^*)$ is the equivalent ellipsoidal axis ratio (Goldsmith and Mason,

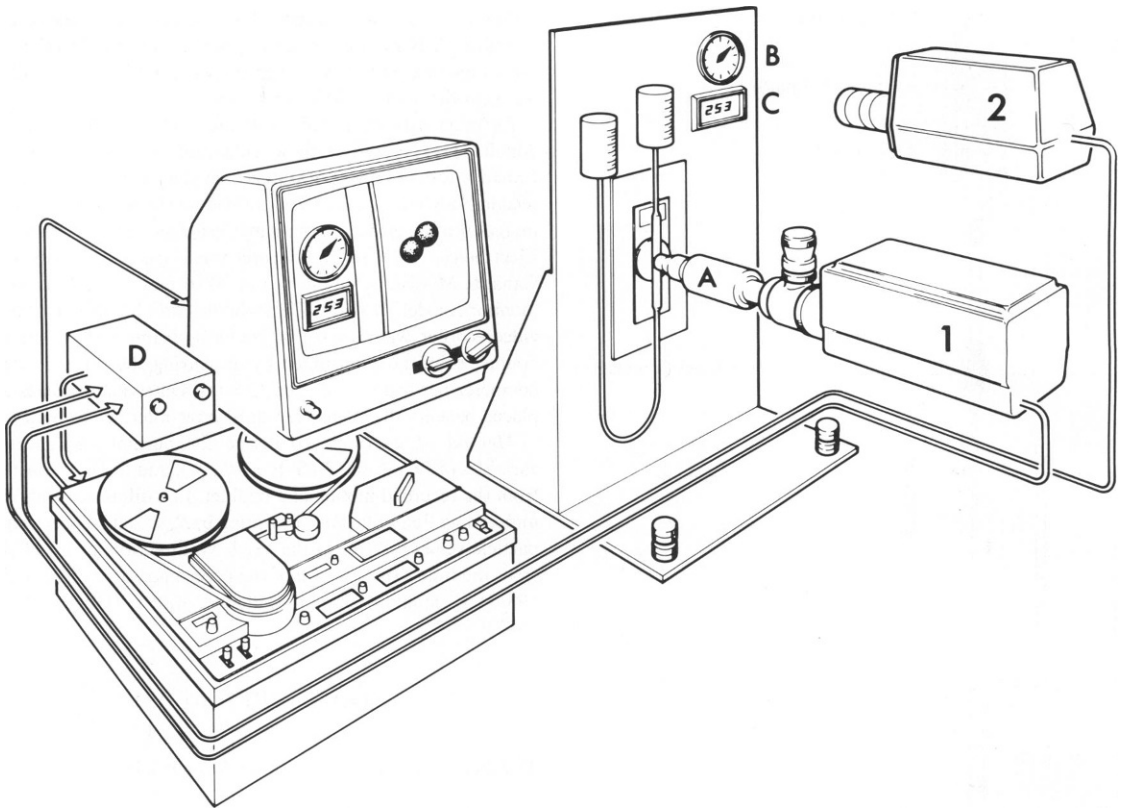

FIGURE 3 Schematic diagram of the double-field video system for simultaneous recording of particle motions, axial position in the microtube, and time. Video camera 1 was attached to the microscope (*A*) recording the doublet rotations while tracking; video camera 2 was focused on an odometer (*B*), indicating the axial distance traveled, and on a digital timer (*C*). By means of the screen splitter (*D*), these two images were displayed on the single TV-monitor, as shown. (After Takamura et al., 1979).

1967) = 1.98 for touching rigid spheres when $r^* = 2b$ (Wakiya, 1971). Values of $r_c(r^*)$ for rigid dumbbells when $r^* > 2b$ have been given by Arp and Mason (1977). In the case of doublets whose axes rotated exclusively in the median plane, $\theta_1 = \pi/2$, (Eqs. 36 and 37 of the preceding paper), the maximum tensile force during each half orbit, F_3, occurs at $\phi_1 = \pi/4$, and the maximal shear force, F_1, occurs at $\phi_1 = 0, \pm \pi/2$. Inspection alone cannot determine the angle at which the bonds are ruptured, as in any event the spheres do not visibly separate until the doublet enters the sector $\pi/4 < \phi_1 < \pi/2$ of the orbit where the forces are tensile (Fig. 1 *b* of the preceding paper). Therefore, it is necessary to assign values of ϕ_1 at breakup. As the increment in F_3 and F_{shear} in each half orbit was very small, it seemed reasonable to assume that the breakup occurred at the maximum value of F_3 and F_{shear} for the immediately preceding half orbit, and these were the values used in Eqs. 1 and 2 respectively.

In the case of doublets rotating in orbits having $C < \infty$, the doublet axis always appeared foreshortened, the measured length of the doublet in the x_2x_3 plane, $l'(\phi_1) < 4b$, θ_1 being a minimum at $\phi_1 = 0$, and a maximum at $\phi_1 = \pi/2$ (Eq. 6). Here, the procedure was to calculate θ_1 at $\phi_1 = 0$ using the relation $\sin\theta_1 = [l'(\phi_1)/2b] - 1$. By substituting this value into Eq. 6, the orbit constant C was obtained and hence θ_1 at any ϕ_1. Again, it was assumed that breakup occurred when F_3 was maximal, hence ϕ_1 and θ_1 were chosen so that $\sin^2\theta_1 \sin 2\phi_1$ was at a maximum. Similarly, for the shear force, $F_{shear} = (F_1^2 + F_2^2)^{1/2}$, for which θ_2 and ϕ_2, calculated from the relations $\cos\theta_1 = \sin\theta_2 \sin\phi_2$, $\sin\theta_1 \cos\phi_1 = \cos\theta_2$ and $\sin\phi_1 \sin\theta_1 = \sin\theta_2 \cos\phi_2$, were chosen so as to maximize the expression $[(\cos 2\theta_2 \cos\phi_2)^2 + (\cos\theta_2 \sin\phi_2)^2]^{1/2}$.

The viscosity of a sample of flow suspension was determined in a thermostated Cannon-Ubbelhode capillary viscometer at 21, 24, and 27°C. The temperature shown by a thermometer placed on the microtube glass slide was recorded after each breakup and the viscosity derived by interpolation.

Period of Rotation

Doublets were also tracked and videotaped in steady flow to obtain mean values of the dimensionless period of rotation, TG. These experiments were carried out in 109- and 145-μm diameter tubes. When a doublet entered the flow tube, the height of the collecting reservoir was lowered by 5–30 mm to produce flow at centerline velocities from 100 to 600 $\mu m\ s^{-1}$ and wall shear rates from 2.3 to 13.5 s^{-1}. The doublets were then tracked along the whole length of the tube, over 50–150 rotations, depending on the particle radial position in the tube. Both doublets in and out of the median plane were followed. Their radial position was obtained by measuring the centerline velocity in the tube immediately after tracking the doublet:

$$\frac{R}{R_o} = \left(1 - \frac{u_3(R)}{u_3(0)}\right)^{1/2}. \tag{7}$$

The centerline velocity was determined by following and videotaping a single red cell sphere flowing along the tube axis. During the time required to track a doublet and centerline sphere (<10 min), the volume flow rate (between 2 and 13 $\mu l\ h^{-1}$) remained measurably constant: the cross-sectional areas of the reservoirs were ~80 mm^2; the reservoir height difference thus decreased from 0.05 to 0.3 mm h^{-1}, or ~1% of the initial value. Doublets whose centers of rotation were closer than one diameter (12.8 μm) from the wall, i. e., $R/R_o > 0.76$ and 0.82, and $u_3(R)/u_3(0) < 0.42$ and 0.32 respectively, were not used in the calculation of the mean TG, as it was known that the vessel wall retards both the translational and rotational velocity of particles moving in its vicinity (Cox and Mason, 1971).

In the experiments, the mean particle velocity, $v_3(R)$, and period of rotation, T, were determined every five rotations (from 0.5 to 4 mm

travel) by playback of the videotape of the doublet motions. Over these distances, and corresponding traveling times from 5 to 15 s, the maximum fluctuations in $R \simeq 2$ μm, i. e., <2% of the wall shear rate at the lowest flow rate. The observed variation in TG between sets of five rotations was generally less than 2% of the mean value, except when a three-body collision occurred, in which case measurements during one rotation before and after the collision were discarded. The centerline velocity was determined over successive 5-mm travel and a mean value calculated. The shear rate of the undisturbed fluid at the doublet center of rotation was calculated from the experimentally determined radial position, using Eq. 4.

EXPERIMENTAL ERROR

Location of Median Plane

It is estimated that errors of ±5 μm were made in deviations from the median plane of the microtube. The depth of focus is known to be approximately ±3 μm, and all images were not perfectly sharp. In the range $0.7R_0 < R < 0.9R_0$ this error would underestimate R by up to 0.35%, but $G(R)$ by as much as 2.5% at large R.

Radial Position of Cells

There is apparent radial displacement of cells because of refraction of light beams. This is known to be <2% at $R < 0.9R_0$ (Goldsmith and Marlow, 1972); nonetheless, this could cause overestimation of $G(R)$ by ~20% at very large R. Few doublet breakups were analyzed at $R > 0.85R_0$, i e., with the center of rotation <13 μm from the wall. Those that were analyzed gave values of the shear and normal forces that were not distinguishable from the remainder of the data set.

Image Distortion

There is additional error of up to 7% introduced by the distortion of the image by the camera. This distortion was partly circumvented by usually restricting analysis to the central 25% of the video screen where distortion was least. The distortion was calibrated horizontally and vertically in micron increments by use of a micrometer scale; thus, tables of distortion factors were generated. The raw experimental data were then multiplied by distortion factors before their manipulation in calculations.

Error in Velocity

Doublet breakup. Doublet velocity was measured over periods of up to 0.5 s, during which a doublet would undergo an increase in velocity of ~6.25 μm s^{-1}. At lower $u_3(R)$ this would be a significant increase. Because the acceleration was constant, it was hoped that error was obviated by choosing an 0.5-s sequence in which breakup occurred at the midpoint, which would average and thus cancel the error.

Doublet rotation. Due to the depth of focus, it was possible that when determining a centerline velocity the sphere being tracked was not exactly at the tube axis and hence its velocity $<u_3(0)$. It is estimated that this error would not exceed 2% since during the time of tracking, spheres with velocities $<0.98u_3(0)$ would be overtaken by particles at the axis, in which case a new measurement would be made. A 2% error in $u_3(0)$ leads to a 1% underestimate in R (Eq. 7), and hence a 3% underestimate in $G(R)$ (Eq. 4) and in TG.

RESULTS AND DISCUSSION

Periods of Rotation

Data were obtained for populations of 51 and 75 doublets respectively at two of the four antiserum concentrations used in the breakup studies: 0.733% in 67% glycerol, and 2.404% in 70% glycerol. The work, which involved analysis of more than 8,000 individual rotational orbits to calculate the mean dimensionless periods of rotation for all the doublets, $\overline{TG}$, was facilitated by entering the particle position and time as read from the videomonitor directly into a microcomputer.

The results are shown in Fig. 4 as histograms of the number distribution in $\overline{TG}$ for each population of doublets, and are summarized in Table I which gives the mean $\overline{TG}$ and the mean relative radial distances, $\overline{R}/R_0$, at each antiserum concentration as well as their values within three or four ranges of increasing shear stress. It is evident from the figure that at both antiserum concentrations there was a fairly narrow distribution in $\overline{TG}$ about the value of 15.64, predicted for rigidly-linked doublets whose surfaces are separated by a distance $h = 0.006$b, that estimated for doublets of red cell spheres crosslinked by IgM antibody (Tha and Goldsmith, 1986). At this value of h/b, the predicted TG for a doublet of freely-rotating spheres is 18.73 (Arp and Mason, 1977). Only three doublets were observed to have $\overline{TG}$ greater than 16.5. Analysis of the 18 doublets with $\overline{TG}$ between 16.0 and 16.5 revealed that 13 of them were situated at radial distances <16 μm from the wall. In fact, a significant correlation between high $\overline{TG}$ and

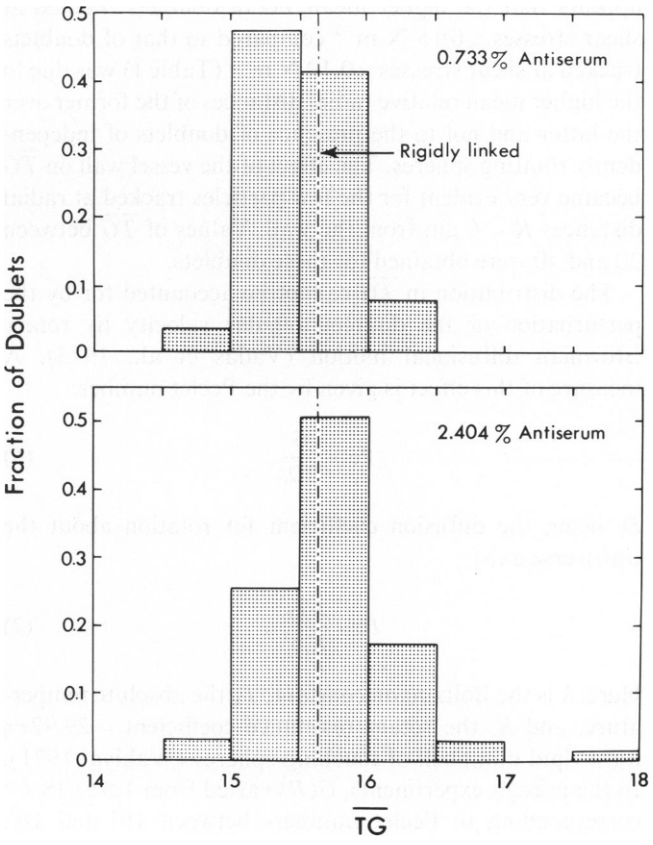

FIGURE 4 Histograms of the number distribution in $\overline{TG}$ within populations of 51 to 75 doublets of red cell spheres in aqueous glycerol suspensions containing antiserum at 0.733 and 2.404%, vol/vol, respectively. The dashed line is drawn at $TG = 15.64$, the value for rigidly-linked doublets of spheres with surfaces at a distance $h = 0.006$b.

TABLE I
SUMMARY OF $\overline{TG}$ VALUES

Antiserum	n	No. of rotations	Range of shear stress	Mean $\overline{TG} \pm$ SD	Mean $\overline{R}/R_o \pm$ SD
% vol/vol			Nm^{-2}		
0.733	25	1,327	0.017–0.100	15.45 ± 0.30*	0.650 ± 0.096‡
	8	345	0.101–0.150	15.40 ± 0.45	0.547 ± 0.069
	18	1,345	0.151–0.253	15.65 ± 0.26*	0.708 ± 0.097‡
	Total 51	3,017	0.017–0.253	15.50 ± 0.33	0.655 ± 0.112
2.404	19	1,240	0.026–0.100	15.50 ± 0.24§	0.677 ± 0.110‖
	17	1,012	0.101–0.150	15.67 ± 0.75	0.612 ± 0.100
	20	1,436	0.151–0.200	15.73 ± 0.38	0.656 ± 0.088
	19	1,734	0.200–0.265	15.81 ± 0.37§	0.734 ± 0.047‖
	Total 75	5,422	0.026–0.265	15.69 ± 0.48	0.672 ± 0.091

*$P < 0.02$.
‡$P < 0.04$.
§$P < 0.001$.
‖$P < 0.03$.

radial position was found: the mean $\overline{TG}$ for doublets tracked at radial distances ≤ 1.5 particle diameters (19.2 μm) from the wall (15.78±0.27 and 15.84±0.45 at 0.733 and 2.404% antiserum, respectively) was significantly higher ($P < 0.001$) than that for the rest of the population (15.37±0.25 and 15.47±0.43, respectively). It thus appears that the higher mean $\overline{TG}$ of doublets tracked at shear stresses >0.15 N m^{-2} compared to that of doublets tracked at shear stresses <0.10 N m^{-2} (Table I) was due to the higher mean relative radial distances of the former over the latter and not to the presence of doublets of independently rotating spheres. The effect of the vessel wall on $\overline{TG}$ became very evident for the few particles tracked at radial distances $R < 6$ μm from the wall. Values of $\overline{TG}$ between 20 and 40 were obtained for these doublets.

The distribution in $\overline{TG}$ cannot be accounted for by the perturbation of the doublet angular velocity by rotary Brownian diffusional motion (Vadas et al., 1973). A measure of this effect is given by the Peclet number:

$$\mathrm{Pe} = \frac{G}{2D_r}, \tag{6}$$

D_r being the diffusion coefficient for rotation about the transverse axis:

$$D_r = \frac{kT_K}{K_r b^3}. \tag{7}$$

Here, k is the Boltzmann constant, T_K the absolute temperature, and K_r the rotary resistance coefficient = $29.92\pi\eta$ for a rigid dumbbell of touching spheres (Wakiya, 1971). In the present experiments, $G(R)$ varied from 1.5 to 18 s^{-1} corresponding to Peclet numbers between 10^4 and 10^5. Results of Monte Carlo calculations (Takamura et al., 1981*a*) show that at such high Pe the variation in TG from orbit to orbit is negligibly small. It is more likely the experimental error in the measurement of $u_3(0)$ which accounts for the values of $\overline{TG} < 15.3$ obtained for 20 and 13% of doublets at 0.733 and 2.404% antiserum, respectively, and the wall effect which accounts for the doublets having $\overline{TG}$ between 16.0 and 16.5. A further source of error is a possible slight departure from sphericity of the red cells, thereby producing doublets having particle axis ratios $\neq 2.0$ which rotate as prolate spheroids with $r_e \neq 1.98$ and $TG \neq 15.64$. Thus, a doublet of two oblate spheroids with $r_e = 1.95$ would have $TG = 15.47$ (Eq. 7 of the preceding paper). As regards the three doublets having $\overline{TG} > 16.5$, it is likely that they belong to a class of aggregates (<1% of all doublets) formed during glutaraldehyde fixation in which surfaces became linked by small fibers and cell debris. These doublets have recently been studied using micropipette manipulation (Tha and Evans, personal communication) and it was shown that the individual red cell spheres are capable of some independent mobility. Flexible doublets of 2–4 μm latex spheres in dilute electrolytes containing cationic polyelectrolyte have also been observed (Takamura et al., 1981*b*) and were modeled as flexible dumbbells linked by elastomer filaments (Adler et al., 1981). Experiments using macroscopic models of such particles showed that $\overline{TG}$ (>16) increased with increasing shear stress and h (Takamura et al., 1981*c*).

We therefore conclude that, apart from a very few flexible dumbbells, red cell spheres crosslinked by antiserum rotate as rigidly-linked doublets.

Forces of Separation

Antiserum concentration. Based on the above conclusion, the forces of separation at four different antiserum concentrations computed from Eqs. 1 and 2 are shown in Figs. 5 and 6, and the mean values given in Table II. There is considerable overlap in their ranges; however, the difference in the means is statistically significant, with the exception of the F_{shear} values for the two middle concentrations which was of borderline significance. Clearly, there is

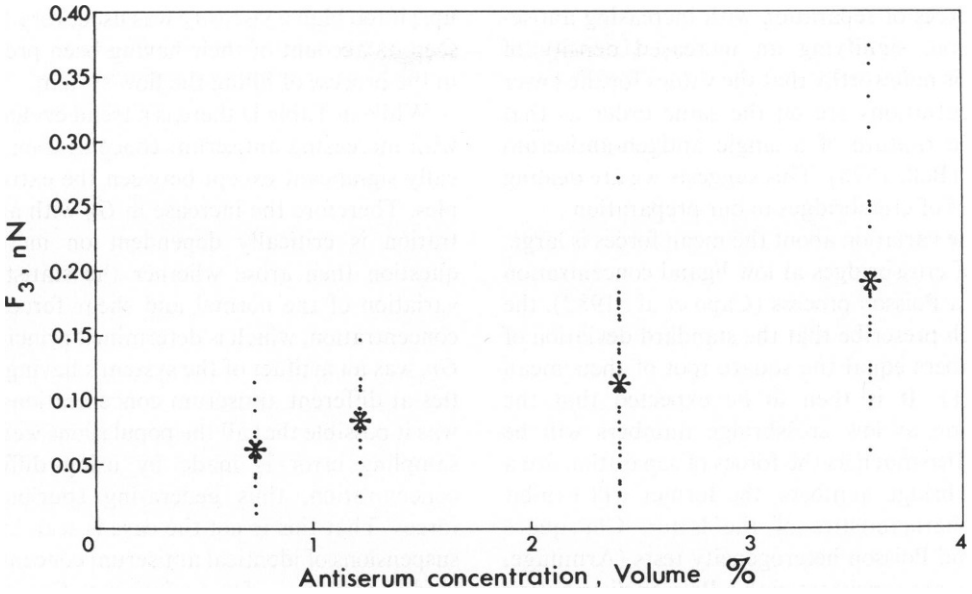

FIGURE 5 Plot of the normal force of separation, F_3, as a function of the antiserum concentration. The stars represent the mean values given in Table II; the differences between all pairs of means are statistically significant.

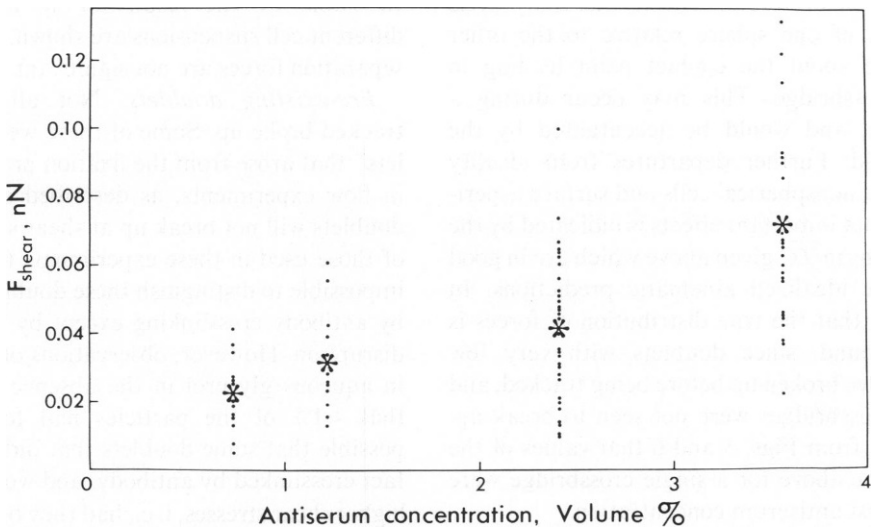

FIGURE 6 Plot, as in Fig. 5, of the shear force of separation, F_{shear}. Here, the differences between the pair of mean values at 1.22 and 2.4% vol/vol of antiserum are not statistically significant. It should be noted that the above values were obtained from the same raw data as those in Fig. 5. Differences in the distribution of points at a given antiserum concentration between the two figures arise from the different trigonometric components in Eqs. 1 and 2.

TABLE II
EFFECT OF ANTISERUM CONCENTRATION ON FORCES OF SEPARATION

Antiserum	n	G	η	$G\eta$		F_3		F_{shear}	
% vol/vol		*s^{-1} ± SD*	*mPa s ± SD*	*N m^{-2} ± SD*		*nN ± SD*		*nN ± SD*	
0.733	16	21.88 ± 9.51	14.4 ± 0.3	0.315 ± 0.136		0.060 ± 0.028		0.023 ± 0.010	
					$P < 0.05$		$P < 0.05$		$P < 0.05$
1.217	17	28.31 ± 16.12	17.6 ± 0	0.497 ± 0.283		0.083 ± 0.032		0.035 ± 0.017	
					$P < 0.10$		$P < 0.05$		$P < 0.10$
2.404	43	31.33 ± 14.72	20.0 ± 2.9	0.619 ± 0.278		0.112 ± 0.054		0.044 ± 0.019	
					$P < 0.001$		$P < 0.001$		$P < 0.001$
3.563	28	35.57 ± 13.60	27.6 ± 0.4	0.981 ± 0.378		0.197 ± 0.083		0.072 ± 0.029	

an increase in forces of separation with increasing antiserum concentration, signifying an increased density of crosslinkages. It is noteworthy that the values for the lower antiserum concentrations are on the same order as that predicted for the rupture of a single antigen-antiserum bond: ~0.04 nN (Bell, 1978). This suggests we are dealing with low numbers of crossbridges in our preparation.

In our data, the variation about the mean forces is large. The formation of crossbridges at low ligand concentration is thought to be a Poisson process (Capo et al., 1982), the statistics of which prescribe that the standard deviation of crossbridge numbers equal the square root of their mean (Armitage, 1971). It is then to be expected that the standard deviation at low crossbridge numbers will be relatively large. Inasmuch as the forces of separation are a function of crossbridge numbers, the former will exhibit the statistical characteristics of the latter. Chi-square goodness of fit and Poisson heterogeneity tests (Armitage, 1971) on our data are consistent with a Poisson distribution and a separation force for a single crossbridge of 0.024 nN for F_3 and 0.009 nN for F_{shear}. However, both theoretical and experimental departures from ideality will affect the frequency distribution of forces. The former may arise because of rotation of one sphere relative to the other setting up a torque about the contact point leading to disruption of a crossbridge. This may occur during a three-body collision, and would be accentuated by the nonlinear shear field. Further departures from ideality may arise because of nonspherical cells and surface asperities. That these are not important effects is indicated by the observed distributions in $\overline{TG}$ given above which are in good agreement with the idealized kinematic predictions. In addition, it is likely that the true distribution of forces is wider than that found, since doublets with very few crossbridges may have broken up before being tracked, and some with many crossbridges were not seen to break up. Indeed, it is evident from Figs. 5 and 6 that values of the forces lower than the above for a single crossbridge were obtained at the lowest antiserum concentration.

Shear rate and viscosity. The viscosity of the flow suspension was chosen such that the majority of doublets visualized at a given antiserum concentration would break up within the range of shear stresses that could be generated in the microtube. Preliminary work showed that if too low a viscosity was chosen, there were few doublet breakups; if too high a viscosity was used, very few doublets were seen on account of their having been previously disrupted in the process of filling the flow system.

While in Table II there is a trend evident of increasing G with increasing antiserum concentration, it is not statistically significant except between the extremes of the samples. Therefore the increase in $G\eta$ with antiserum concentration is critically dependent on increases in η. The question then arose whether the statistically significant variation of the normal and shear forces with antiserum concentration, which is determined principally by values of $G\eta$, was an artifact of the system's having different viscosities at different antiserum concentrations; in other words, was it possible that all the populations were the same, but a sampling error is made by using different η at each concentration, thus generating spurious differences in forces. That this is not the case is seen in Table III. Here suspensions of identical antiserum concentration are examined at varying η. The variation of $G\eta$ and F_{shear} and F_3 at different η are not significant. As would be expected, there is a trend of decreasing G with increasing η.

Different cell preparations were used at different times. In Table IV the results of an experiment comparing different cell suspensions are shown. The differences in the separation forces are not significant.

Pre-existing doublets. Not all doublets that were tracked broke up. Some of these were "pre-existing doublets" that arose from the fixation process prior to their use in flow experiments, as described above. Many of these doublets will not break up at shear stresses much in excess of those used in these experiments (data not shown). It is impossible to distinguish these doublets from those formed by antibody crosslinking except by their refractoriness to disruption. However, observations of the tube flow of cells in aqueous glycerol in the absence of antiserum showed that <1% of the particles had formed doublets. It is possible that some doublets that did not break up were in fact crosslinked by antibody, and would have broken up at higher shear stresses, i. e., had they been situated at greater R in the microtube or had η been higher. As there was no difference in mean R of tracked doublets for the samples, the first possibility would have led to an underestimation of G (and F_{shear} and F_3) by the same factor for all samples, consequently not affecting the statistical significance of their differences. The second possibility is suggested by

TABLE III
EFFECT OF SUSPENDING MEDIUM VISCOSITY ON FORCES OF SEPARATION

Antiserum	n	G	η	$G\eta$	F_3	F_{shear}
% vol/vol		*s^{-1} ± SD*	*mPa s ± SD*	*N m^{-2} ± SD*	*nN ± SD*	*nN ± SD*
2.404	11	34.06 ± 17.17	16.9 ± 0.6	0.578 ± 0.296*	0.103 ± 0.048*	0.042 ± 0.022*
2.404	15	33.82 ± 16.56	18.5 ± 0.3	0.626 ± 0.308*	0.119 ± 0.062*	0.045 ± 0.022*
2.404	17	27.35 ± 10.80	23.4 ± 0.4	0.639 ± 0.250*	0.112 ± 0.052*	0.045 ± 0.018*

*No significant difference between any of the three values.

TABLE IV
EFFECT OF DIFFERENT CELL SUSPENSION ON FORCES OF SEPARATION

Antiserum	n	F_3	F_{shear}
% vol/vol		*nN ± SD*	*nN ± SD*
2.404	8	0.104 ± 0.053	0.043 ± 0.024
2.404	35	0.114 ± 0.055	0.044 ± 0.019

Table II, in so far as there is a trend of increasing G with increasing η at higher antiserum concentrations. Although the proportion of doublets not breaking up was not noticeably greater at higher antiserum concentrations, the higher G at these concentrations suggest that had η been higher, more doublets might have broken up. If this were the case, the differences in F_{shear} and F_3 between the different populations would have been greater than calculated.

Some of the doublets crosslinked by fibers or cell debris can be broken up by forces comparable to those prevailing in the experiments. Although a small minority, such doublets would add to the scatter in the values of the separation forces.

Aldehyde fixation. Red cell aggregation is a complex process dependent not only upon the class of antibody, the antigenic determinant, and the thermodynamics of their interaction, but also on the zeta potential of the red cell, its deformability, and the nature of the suspending medium. It is assumed that crosslinking occurs as multivalency of ligand is a requirement. Although anti-B IgG can agglutinate rbc and IgG concentrations are high in hyperimmune sera, it is thought that the principal agglutinator in the conditions of these experiments was IgM. Treatment of the antiserum used with 2-mercapto-ethanol, which cleaves IgM, decreased the agglutination such that it was absent or slight at the dilutions used in our experiments (data not shown). This suggests that the role of IgG was not primary. The efficacy of IgM has been attributed to its being a larger molecule than IgG (van Oss and Absolom, 1983), that can bind to a single cell surface by more than one binding site (Hughes-Jones, 1972).

Antiserum concentrations were chosen to be in the middle range of those causing agglutination of the sphered, hardened rbc. Whereas untreated rbc in buffer will agglutinate massively at low dilutions of these anti-A or -B antisera, and exhibit microscopic agglutination to dilutions of 1/2048 or beyond, hardened cells are known to less readily form large aggregates (Marquardt and Gordon, 1975). This is thought to be on account of the cells' lack of deformability and the immobility of their receptors. A deformable cell is able to increase the area of contact after contact with another cell or substrate has been made (Evans and Parsegian, 1983), whereas a hardened cell has a fixed maximal contact area with another cell, the extent of which is dependent on their configurations. The smaller contact area can cause aggregates to be less stable to mechanical disruption. This instability of cell–cell and cell–substrate contacts has been found experimentally for a variety of hardened cells and agglutinating agents (Capo et al., 1982; Trommler et al., 1985; Knox et al., 1977).

The process of hardening an rbc with glutaraldehyde does not alter greatly its agglutinability other than as described above. Glutaraldehyde acts principally on proteins, causing crosslinking (Peters and Richards, 1977); its effect on carbohydrate and lipid moieties is thought to be minimal, and it alters protein conformation less than most other fixatives (Lenard and Singer, 1968). The A and B blood group antigens are oligosaccharides bound to intrinsic membrane proteins or glycolipids (Hakomori, 1981), and thus no alteration in their structure would be expected. Indeed, many of the anti-A and -B binding studies have utilized aldehyde-fixed cells (Economidou et al., 1967). The zeta potential of the red cell, a known variable in agglutination, may be increased by $\leq 10\%$ in glutaraldehyde-fixed cells at neutral pH (Vassar et al., 1972).

CONCLUDING REMARKS

These experiments have provided direct measurements of the forces necessary to disrupt the antibody-mediated adhesion of two red blood cells. The results are within the range of the published data for the force required to separate red cells agglutinated by lectin (Evans and Leung, 1984).

The process of agglutination is known often not to be reversible in a thermodynamic sense: the forces required to disaggregate cells can be much greater than would be predicted by the free energy reduction of contact formation (Evans and Parsegian, 1983). This behavior is thought to follow from receptor mobility (Bell et al., 1984), membrane elastic properties (Evans, 1985*a*, *b*) and cell viability. None of these obtain in the present instance. However, it is possible that, despite their being inert, subsequent chemical reactions occur between sphere surfaces. It is also possible that the separation forces are acting to uproot the antigenic molecules from the cell membrane rather than breaking antigen-antibody bonds. We think the former unlikely, as glutaraldehyde rigidifies the membrane protein matrix.

The values of F_{sep} obtained show that the number of crossbridges between cells are few. It seems probable, therefore, that the technique will provide a means of measuring the strength of a single crossbridge. However, owing to the heterogeneity of our antiserum and the absence of uptake data, no definitive statements can be made about the antibody-antigen bond strength, other than its range being $\leq 10^{-11}$ N. The use of monoclonal antibodies could circumvent some of these uncertainties.

The authors gratefully acknowledge the technical assistance of Samira Spain and Carolyn Timm, the very helpful comments of the referees, and the many useful discussions with David Bell and Drs. Theo van de Ven and Raymond Cox.

This work was supported by Grant MT-1835 from the Medical Research Council of Canada.

Received for publication 9 December 1985 and in final form 20 June 1986.

REFERENCES

Adler, P. M., K. Takamura, H. L. Goldsmith, and S.G. Mason. 1981. Particle motions in sheared suspensions. XXX. Rotations of rigid and flexible dumbbells (theoretical). *J. Colloid Interface Sci.* 83:502–515.

Armitage, P. 1971. Statistical Methods in Medical Research. Blackwell Scientific Publications, Oxford. 504 pp.

Arp, P. A., and S. G. Mason. 1977. The kinetics of flowing dispersions. VIII. Doublets of rigid spheres (theoretical). *J. Colloid Interface Sci.* 61:21–43.

Bell, G. I. 1978. Models for the specific adhesion of cells to cells. *Science (Wash. D.C.).* 200:618–627.

Bell, G. I., M. Dembo, and P. Bongrand. 1984. Cell adhesion. Competition between nonspecific repulsion and specific binding. *Biophys. J.* 45:175–183.

Capo, C., F. Garrouste, A. -M. Benoliel, P. Bongrand, A. Ryter, and G. I. Bell. 1982. Concanavalin-A-mediated thymocyte agglutination: a model for a quantitative study of cell adhesion. *J. Cell Sci.* 56:21–48.

Cox, R. G., and S. G. Mason. 1971. Suspended particles in fluid flow through tubes. *Annu. Rev. Fluid Mech.* 3:291–316.

Economidou, J., N. C. Hughes-Jones, and B. Gardner. 1967. Quantitative measurements concerning A and B antigen sites. *Vox Sang.* 12:321–328.

Evans, E. A. 1985*a*. Detailed mechanics of membrane-membrane adhesion and separation. I. Continuum of molecular crossbridges. *Biophys. J.* 48:175–183.

Evans, E. A. 1985*b*. Detailed mechanics of membrane-membrane adhesion and separation. II. Discrete kinetically trapped molecular crossbridges. *Biophys. J.* 48:185–192.

Evans, E. A., and A. Leung. 1984. Adhesivity and rigidity of red blood cell membrane in relation to WGA binding. *J. Cell Biol.* 98:1201–1208.

Evans, E. A., and V. A. Parsegian. 1983. Energetics of membrane deformation and adhesion in cell and vesicle aggregation. *Ann. NY Acad. Sci.* 416:13–33.

Goldsmith, H. L., and Jean Marlow. 1972. Flow behaviour of erythrocytes. I. Rotation and deformation in dilute suspensions. *Proc. R. Soc. Lond. B. Biol. Sci.* 181:351–384.

Goldsmith, H. L., and S. G. Mason. 1962. The flow of suspensions through tubes. I. Single spheres, rods and discs. *J. Colloid Sci.* 17:448–476.

Goldsmith, H. L., and S. G. Mason, 1967. The microrheology of dispersions. *In* Rheology: Theory and Applications. Vol. 4. F. R. Eirich, editor. Academic Press, Inc. New York. 85–250.

Goldsmith, H. L., and S. G. Mason. 1975. Some model experiments in hemodynamics. V. Microrheological techniques. *Biorheology.* 12:181–192.

Goldsmith, H. L., P. Gold, J. Shuster, and K. Takamura. 1982. Interactions between sphered human red cells in tube flow: technique for measuring the strength of antigen-antibody bonds. *Microvasc. Res.* 23:231–238.

Goldsmith, H. L., O. Lichtarge, M. Tesssier-Lavigne, and S. Spain. 1981. Some model experiments in hemodynamics. VI. Two-body collisions between blood cells. *Biorheology.* 18:531–555.

Hakomori, S. -I. 1981. Blood group ABH and Ii antigens of human erythrocytes: chemistry, polymorphism and their developmental change. *Semin. Hematol.* 18:39–62.

Hughes-Jones, N. C. 1972. The attachment of IgG molecules on the red cell surface. *Haematologia.* 6:269–274.

Jeffery, G. B. 1922. On the motion of ellipsoidal particles immersed in a viscous fluid. *Proc. R. Soc. Lond.* A. 102:161–179.

Knox, R. J., F. J. Nordt, G. V. F. Seaman, and D. E. Brooks. 1977. Rheology of erythrocyte suspensions: dextran-mediated aggregation of deformable and non-deformable erythrocytes. *Biorheology.* 14:75–84.

Lenard, J. and S. J. Singer. 1968. Alteration of the conformation of proteins in red blood cell membranes and in solution by fixatives used in electron microscopy. *J. Cell Biol.* 37:117–121.

Marquardt, M. D., and J. A. Gordon, 1975. Glutaraldehyde fixation and the mechanism of erythrocyte agglutination by concanavalin A and soybean agglutinin. *Exp. Cell Res.* 91:310–316.

Peters, K., and F. M. Richards. 1977. Chemical cross-linking: reagents and problems in studies of membrane structure. *Annu. Rev. Biochem.* 46:523–551.

Takamura, K., H. L. Goldsmith, and S. G. Mason. 1979. The microrheology of colloidal dispersions. IX. Effects of simple and polyelectrolytes on rotation of doublets of spheres. *J. Colloid Interface Sci.* 72:385–400.

Takamura, K., T. G. M. van de Ven, and S. G. Mason. 1981*a*. The microrheology of colloidal dispersions. XI. Measured effects of Brownian motion on the rotation of doublets of spheres in shear flow. *J. Colloid Interface Sci.* 82:384–393.

Takamura, K., H. L. Goldsmith, and S. G. Mason. 1981*b*. The microrheology of colloidal dispersions. XIII. Trajectories of orthokinetic pair-collisions of latex spheres in a cationic polyelectrolyte. *J. Colloid Interface Sci.* 82:190–202.

Takamura, K., P. M. Adler, H. L. Goldsmith, and S. G. Mason. 1981*c*. Particle motions in sheared suspensions. XXXI. Rotations of rigid and flexible dumbbells (experimental). *J. Colloid Interface Sci.* 83:516–530.

Tha, S. P., and H. L. Goldsmith. 1986. Interaction forces between red cells agglutinated by antibody. I. Theoretical. *Biophys. J.* 50:2009–2016.

Trommler, A., D. Gingell, and H. Wolf. 1985. Red blood cells experience repulsion but make molecular adhesions with glass. *Biophys. J.* 48:835–841.

Vadas, E. B., H. L. Goldsmith, and S. G. Mason. 1973. The microrheology of colloidal dispersions. I. The microtube technique. *J. Colloid Interface Sci.* 43:630–648.

Van Oss, C. J., and D. R. Absolom. 1983. Zeta potentials, van der Waals forces and hemagglutination. *Vox Sang.* 44:183–190.

Vassar, P. S., J. M. Hards, D. E. Brooks, B. Hagenberger, and G. V. F. Seaman. 1972. Physicochemical effects of aldehyde fixation on the human erythrocyte. *J. Cell Biol.* 53:809–818.

Wakiya, S. 1971. Slow motion in shear flow of a doublet of two spheres in contact. *J. Phys. Soc. Jpn.* 31:1581–1587. (errata [1972] 33:278)